

PRODUCTION AND DIFFUSION OF MUONIUM IN POWDERED SILICA

by

GLEN MURRAY MARSHALL  
B.Sc., McGill University, 1974

A THESIS SUBMITTED IN PARTIAL FULFILLMENT OF  
THE REQUIREMENTS FOR THE DEGREE OF  
MASTER OF SCIENCE

in  
THE FACULTY OF GRADUATE STUDIES  
(Physics)

We accept this thesis as conforming  
to the required standard

THE UNIVERSITY OF BRITISH COLUMBIA  
December, 1976

© Glen Murray Marshall, 1976

In presenting this thesis in partial fulfilment of the requirements for an advanced degree at the University of British Columbia, I agree that the Library shall make it freely available for reference and study.

I further agree that permission for extensive copying of this thesis for scholarly purposes may be granted by the Head of my Department or by his representatives. It is understood that copying or publication of this thesis for financial gain shall not be allowed without my written permission.

Department of Physics

The University of British Columbia  
2075 Wesbrook Place  
Vancouver, Canada  
V6T 1W5

Date

Dec. 31, 1976

ABSTRACT

The first direct observation of the atomic state of the muon (muonium) in a finely powdered sample of  $\text{SiO}_2$  (silica) is reported, with evidence of muonium diffusion into a vacuum. The formation technique, first used in the study of the positron atomic state (positronium), has been extended and modified to suit the particular requirements of a beam of surface muons presently available at TRIUMF. Some emphasis is placed on a description of the muon beam, its operation, and the problems inherent in the successful use of these low energy, nearly monokinetic, polarized particles. The basic method of MSR (muonium spin rotation) as it applies to the experimental circumstances is reviewed. The use of powder targets of this kind is examined in the context of possible experiments in weak interactions, diffusion studies, and gas chemistry.

## TABLE OF CONTENTS

- I. Introduction
- II. Related Phenomena
  - A. Experimental Problem
  - B. Other Experiments
- III. The Positronium Analogy
  - A. Pioneering Powder Experiments
  - B. Techniques of Orthopositronium Observation
    - 1. Angular correlation
    - 2. Lifetime
    - 3. Gamma spectrum analysis
  - C. Testing the Powder Samples
    - 1. Experimental design
    - 2. Data analysis
    - 3. Results
- IV. The TRIUMF Experiment
  - A. The Source of Muons
    - 1. General
    - 2. The TRIUMF M9 channel
    - 3. Surface muons
    - 4. Detection of low energy muons
    - 5. Tuning for surface muons
  - B. The MSR Time Spectrum
    - 1. Rotation
    - 2. Relaxation
    - 3. Spectral form
    - 4. Typical muonium and muon spectra
  - C. Apparatus
    - 1. Precession cart
    - 2. Electronics and data collection
  - D. Muonium in Silica Powder
    - 1. Quenching technique
    - 2. Results
- V. Evaluation; Diffusion of Muonium into a Vacuum
  - A. Qualitative Assessment
  - B. Quantitative Consequences of the Observed Muonium Asymmetry
  - C. Applications in Future Experiments
    - 1. Feasibility of an antimuonium experiment
    - 2. Diffusion studies
    - 3. Chemistry of gases
- VI. Bibliography

LIST OF TABLES

Title	Page
I. Lepton Number Assignment Scheme	2a
II. Additive Muon Number Assignment Scheme	2b
III. Multiplicative Muon Number Assignment Scheme	2b
IV. Positronium Experimental Results	13a
V. Muonium Experimental Results	24a

LIST OF FIGURES

Title	Page
1. Positronium Annihilation	10a
2. Positronium Annihilation in Quartz Powder	12a
3. M9 Beam Schematic	15a
4. Surface Muon Range Curve	17a
5. Positron Energy Spectrum and Asymmetry Parameter	18a
6. Helicities in $\pi^+ \rightarrow \mu^+ \rightarrow e^+ \bar{\nu}_e$ Decay	18b
7. Muonium in Fused Quartz (4.2 Gauss)	20a
8. Asymmetry of Muons in Carbon Tetrachloride (75 Gauss)	20b
9. Muon Precession in Copper (75 Gauss)	20c
10. Precession Apparatus	21a
11. MSR Electronics and Logic	22a
12. Muonium in Silica Powder at $10^{-6}$ Torr (2.5 Gauss)	24b
13. Muonium in Silica Powder at 0.05 Torr (2.5 Gauss)	24c
14. Muonium in Silica Powder at 0.15 Torr (2.5 Gauss)	24d
15. Muonium in Silica Powder at 0.40 Torr (2.5 Gauss)	24e
16. Relaxation Rate as a Function of Oxygen Pressure	26a

## ACKNOWLEDGEMENT

Upon presentation of this thesis, I would like to thank those who have assisted in the research and preparation behind it. In particular, I am grateful to Dr. J. B. Warren for his suggestions regarding the experimental techniques and his advice in the writing of the text; to the entire TRIUMF MSR Group, whose time and effort have created a fine MSR facility; and to Mr. George Clark, for his talents in the design and construction of the hardware necessary for a successful experiment.

## I. Introduction

With the advent of the so-called meson factories, the use of the muon as a tool for investigating properties of materials and details of interactions becomes a practical, illuminating pursuit. Such attributes as long lifetime ( $\sim 2.2 \mu\text{sec}$ ), magnetic moment, asymmetric decay, and point-like structure coupled with the availability of highly polarized beams make the muon spin research ( $\mu\text{SR}$ ) method (and MSR, its muonium counterpart) unique, although not without analogue, in studying some properties of a variety of solids, liquids, and gases.

Muonium ( $\mu^+e^-$ , denoted also as M) is often regarded conceptually as a light isotope of atomic hydrogen, of mass about one-ninth that of the heavier atom. Since the muon is still heavier than the electron by over 200 times, the atomic size is not appreciably different from hydrogen, in contrast to positronium, where the mass of the positive particle is the same as that of the electron. Positronium was at one time considered as a light isotope of hydrogen, but due to large size (twice the Bohr radius) and mass differences, the validity of this approach is far from universal. Positronium phenomena are in general difficult to interpret vis-a-vis its interactions with a medium in any phase.

One of the more successful treatments of these phenomena has been the determination of positronium diffusion constants by stopping positrons in finely powdered samples of  $\text{MgO}$ ,  $\text{Al}_2\text{O}_3$ , and  $\text{SiO}_2$ . (Brandt and Paulin, 1968) In principle, the MSR (muonium spin rotation) method enables the same type of experiment to be performed with muons. Moreover, a powder may provide muonium in vacuum, enabling further experiments on this system.

## II. Related Phenomena

The muon has long been regarded as a heavy electron because it does not interact strongly with nuclear matter. This is a basic quality of the lepton family, which also includes neutrinos and antineutrinos. It was not until more recently that the existence of two types of neutrino-antineutrino pairs was established (Danby et al, 1962), now referred to as electron ( $\nu_e, \bar{\nu}_e$ ) and muon ( $\nu_\mu, \bar{\nu}_\mu$ ) neutrinos.

The individual identity of the muon has since been more firmly underlined by the need for a separate conservation law for what is termed as muon (or muonic lepton) number, in addition to a lepton conservation law. For instance, processes such as the following are not observed:

$$\begin{aligned}\mu^\pm &\rightarrow e^\pm + \gamma \\ \mu^+ &\rightarrow e^+ + e^- + e^+ \\ \mu^+ + A_z &\rightarrow e^+ + A_z \\ \nu_e + n &\rightarrow \mu^- + p\end{aligned}$$

Each reaction is allowed by conservation of total lepton number  $\Sigma \ell_e$  (see Table I). The physical forbidden nature becomes evident only when the conservation of the sum of muon number  $\Sigma \ell_\mu$  (Table II) is invoked.

In terms of applicability, however, the additive rule is not unique. In fact, a less restrictive law by which the product of a different set of muon numbers must be conserved, as with parity, is consistent with observation (see Table III): also, if such a law were shown to be obeyed, it would have ramifications in the theory of weak interactions, since either scheme, additive or multiplicative, can be deduced by assuming different transformation properties of the neutrino field.

Particle	Lepton Number
$e^{-}, \nu_e$	+1
$e^{+}, \bar{\nu}_e$	-1
$\mu^{-}, \nu_\mu$	+1
$\mu^{+}, \bar{\nu}_\mu$	-1
Hadrons	00

TABLE I. LEPTON NUMBER ASSIGNMENT SCHEME

Particle	Muon Number
$e^{-}, \nu_e$	-1
$e^{+}, \bar{\nu}_e$	+1
$\mu^{-}, \nu_{\mu}$	+1
$\mu^{+}, \bar{\nu}_{\mu}$	-1
Hadrons	0

TABLE II. ADDITIVE MUON NUMBER ASSIGNMENT SCHEME

Particle	Muon Number
$\mu^{\pm}, \nu_{\mu}, \bar{\nu}_{\mu}$	-1
$e^{\pm}, \nu_e, \bar{\nu}_e$	+1
Hadrons	0

TABLE III. MULTIPLICATIVE MUON NUMBER ASSIGNMENT SCHEME

In order to test muon number conservation, one could look for the decay:

$$\mu^+ \rightarrow e^+ + \bar{\nu}_e + \nu_\mu \quad (1)$$

The usual positive muon decay involves  $\nu_e$  and  $\bar{\nu}_\mu$  and is allowed under both schemes, whereas (1) is consistent only with the multiplicative law. Experimentally, detection of neutrinos is difficult at best, and observation of the alternative  $\mu^+$  decay mode is somewhat impractical as a test of conserved quantities (Eichten et al, 1973).

Another test, which in the past has not been possible for reasons which will be explained shortly, is to search for the conversion of muonium into what is termed as antimuonium ( $\mu^- e^+$ , or  $\bar{M}$ ):

$$\mu^+ + e^- \rightarrow \mu^- + e^+$$

In an additive scheme, this interaction is not allowed since  $\Sigma \ell_\mu$  is -2 for  $\bar{M}$  and +2 for  $M$  (Table II). Since  $\Pi \ell_\mu$  is -1 for both  $M$  and  $\bar{M}$  (Table III), the conversion is consistent with the multiplicative scheme.

Obviously, the observation of  $\bar{M}$  in a system initially prepared in the  $M$  state would indicate that the more general parity-like conservation law better describes lepton behavior. It would also indicate the existence of a neutral lepton current in the weak interaction Hamiltonian (Feinberg and Weinberg, 1961).

On the other hand, if no  $\bar{M}$  is observed, one can only set some upper limits. By postulating a specific form for the possible  $M$ - $\bar{M}$  interaction, such as:

$$H = \frac{G}{\sqrt{2}} \bar{\psi}_\mu \gamma_\lambda (1+\gamma_5) \psi_e \bar{\psi}_\mu \gamma^\lambda (1+\gamma_5) \psi_e + H.C. \quad (2)$$

where  $G$  is the  $M$ - $\bar{M}$  coupling constant, the conversion rate can be calculated in terms of  $G/G_V$ . Since  $G_V$ , the usual vector coupling constant, is known very accurately from beta decay, an estimate of  $G$  can be extracted.

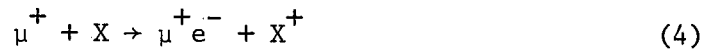
The probability of this interaction is (Feinberg and Weinberg, 1961), in the absence of external fields:

$$P(M \rightarrow \bar{M}) = 2.5 \times 10^{-5} \left( \frac{G}{G_v} \right)^2 \quad (3)$$

Thus, assuming the validity of the interaction (2), and assuming that the multiplicative law does describe nature's selectivity, one can set an upper limit on the coupling constant  $G$ .

### A. The Experimental Problem

According to such calculations, it would seem that an antimuonium experiment is straightforward, but such is not the case. One must prepare muonium from a beam of muons thermalized in the presence of an electron donor, in a chemical reaction of the form:



As shown by Feinberg and Weinberg, the conversion process is drastically altered in the presence of matter, which, from (4), is a necessary condition for the initial formation.

Specifically, the presence of electromagnetic fields breaks the energy degeneracy of the  $M$  and  $\bar{M}$  states by an amount  $\Delta$ , thus reducing the probability of conversion. It is estimated that unless  $\Delta \ll 3 \times 10^{-10}$  eV, the interaction (2) would be quenched beyond observation in the lifetime of muonium. It is further estimated that the lowest order contributions to  $\Delta$  will be of order  $E^3$ , and to lowest order in gradients:

$$\Delta \propto \bar{E} : \bar{\nabla}(E^2)$$

For  $E \ll 10^8$  volts per centimetre,  $\Delta$  is insignificant. The longitudinal magnetic field must be kept to  $< 0.01$  gauss, however, in order that the  $1S (F, F_z) = (1, \pm 1)$  states are not split so much that the conversion is completely quenched.

For muonium in a gas, the conversion probability must be multiplied by the inverse of the collision rate to take into account the environmental effect on  $\Delta$ . At reasonable moderator pressures, ( $\approx 1$  Torr) this effect is great enough to place the experiment beyond feasibility.

## B. Previous Experiments

The interest in a muonium conversion experiment is not new; in fact, at least three attempts, using dissimilar techniques, have been made. None has met with success. They have served only in emphasizing the major difficulty, that of producing the muonium in collisionless space or high vacuum. Each has used a different muon moderator - electron donor combination. The first attempt (Amato et al, 1968) relied on argon gas at atmospheric pressure to stop the muons and supply the electrons. A search for the characteristic argon muonic K<sub>α</sub> X-ray was made, since there should be a high  $\mu^-$  capture rate in an argon-antimuonium collision. The result of the experiment was consistent with zero, and the lowest upper limit that could be established for the M-M<sub>v</sub> coupling constant was  $G < 5800G_v$ . The muonium collision rate severely restricted the probability of conversion. Another experiment (Hofer et al, 1972) has met with no greater success. A beam of pions at 39.5 MeV/c momentum was allowed to decay in flight in a magnetic field parallel to the beam. Some backward emitted muons should then have energies <10 keV. These slow particles would follow a long helical path due to the field and could form muonium in a collision with an argon atom of the low pressure gas environment. The uncharged system would have a radial velocity component and could be detected in a direction perpendicular to the beam. However, no signal attributable to this process has yet been reported.

The third technique (Kendall, 1972) used a 24 MeV/c 100% polarized muon beam stopping in thin platinum foils heated to ~1500°C. Muons diffusing to the foil surface were expected to form muonium and escape into the

vacuum environment. Again, an insignificant amount of muonium was detected (Bowen et al, 1973).

Other similar experiments are in progress at the meson facilities. For instance, LAMPF has received proposals for testing muon behavior in thin gold foils. Several neutrino experiments are also planned there to check lepton conservation from another approach. Yet another experiment is designed to investigate muon conservation laws using  $\mu^-$  capture in nuclei with subsequent electron emission.

### III. The Positronium Analogy

Since hydrogen, muonium, and positronium atoms are all hydrogen-like systems, one would expect some similarity in behavior in a given environment, the main differences arising from size and (reduced) mass effects. However, high flux muon sources in the form of meson factory beamlines have been only recently available, and studies of positive muon behavior are not yet as extensive as those of positrons. Compact sources of isotopes such as  $^{22}\text{Na}$ ,  $^{58}\text{Co}$ , and  $^{64}\text{Cu}$  have long been used to provide positrons in a wide range of experiments (West, 1973). The unravelling of the complex behavior of positronium (Ps) has been slowly advancing, and it seems reasonable to make comparisons and seek information from analogous Ps studies in the first stages of a muonium experimental program.

### A. Pioneering Powder Experiments

The first experiments in which positrons were injected into finely powdered insulator samples showed (Paulin and Ambrosino, 1968) that positronium was produced in the powder grains and could diffuse out to annihilate in the intergranular vacuum. The exact formation process is still not as well understood as, for example, Ps formation in inert gases, but the result was clear: a positron, on slowing in the solid, could diffuse and leave the granule in the form of positronium. This positronium annihilates to three  $\gamma$ -rays with the longer  $\tau_o = 140$  nsec lifetime of the triplet ortho-positronium (o-Ps) state, whereas two shorter lifetime components, both observed in bulk samples, arise from annihilation within the granules. The shorter lifetimes indicate two gamma decay; the first ( $\tau_p \approx 0.4$  nsec) due to in-flight as well as singlet parapositronium (p-Ps) annihilation, the second ( $\tau_{pickoff} \approx 2$  nsec) due to pickoff of electrons from the medium by the bound positron in o-Ps. These lifetimes are shorter than the average time taken to diffuse into the vacuum.

Shortly after the discovery of this effect, it was applied to the problem of determining the diffusion rate of o-Ps in insulating solids such as  $SiO_2$ ,  $Al_2O_3$ , and  $MgO$ . More recently the vacuum lifetime of o-Ps was measured with great accuracy using this diffusion (Gidley et al, 1975), and the results obtained showed some discrepancy with the theoretical predictions of quantum electrodynamics. Thus the technique has proven worthwhile in more than one branch of physics.

## B. Techniques of Orthopositronium Observation

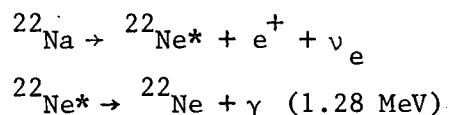
There are three basic approaches to positronium investigations, each with slightly different applications. (West, 1973). They are briefly described here in the context of how they can and have been applied in the studies of insulating powders. (Fig. 1)

### 1. Angular correlation

A parapositronium atom at rest will decay into two  $\gamma$ -rays emitted at  $180^\circ$  to conserve momentum, thus the coincidence rate of two well collimated detectors as a function of angular displacement can show sharp peaking about this angle. In bulk samples this effect is smeared due to the zero-point energy of the atom. In a finely powdered insulator, injected positrons will form both o-Ps and p-Ps, but due to their much longer lifetime the o-Ps atoms diffuse much farther. This is manifested in the appearance of a sharp angular correlation peak as the powder size is reduced to  $< 100 \text{ \AA}$  when the sample is in vacuum in a strong magnetic field. The field mixes the  $m=0$  substates of o-Ps and p-Ps, and leads to two gamma annihilation in the vacuum, where the zero-point energy is small. (Steldt and Varlashkin, 1972).

### 2. Lifetime

In some isotopes the formation of the beta decay positronium leaves the nucleus in an excited state which promptly ( $< 10^{-11}$  sec) emits a gamma ray of specific energy, as in the process:



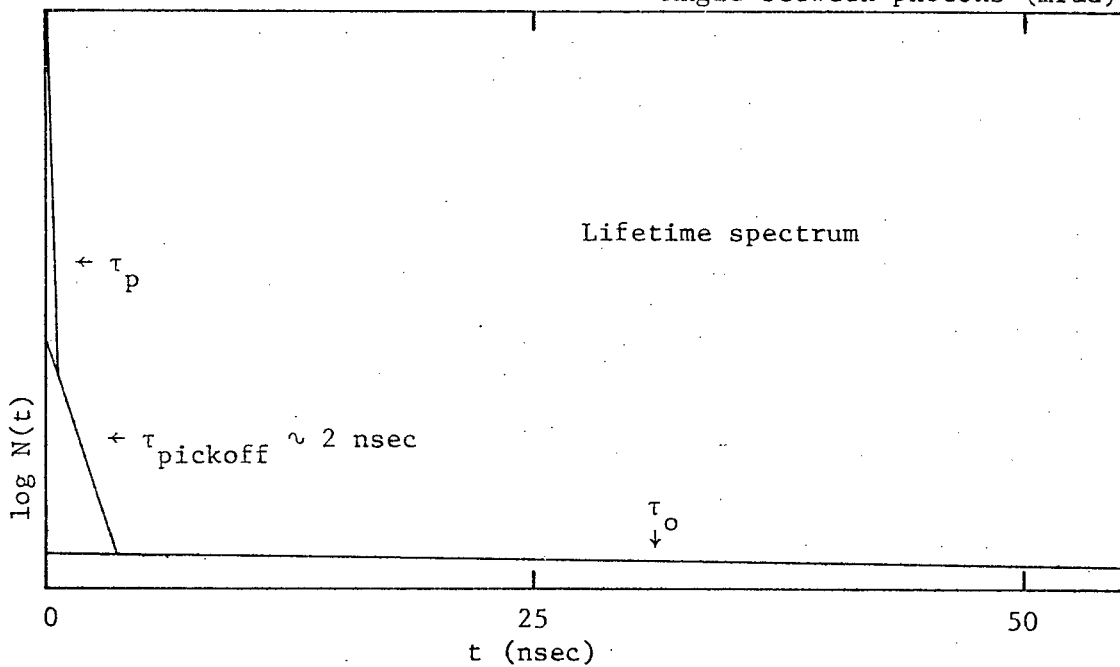
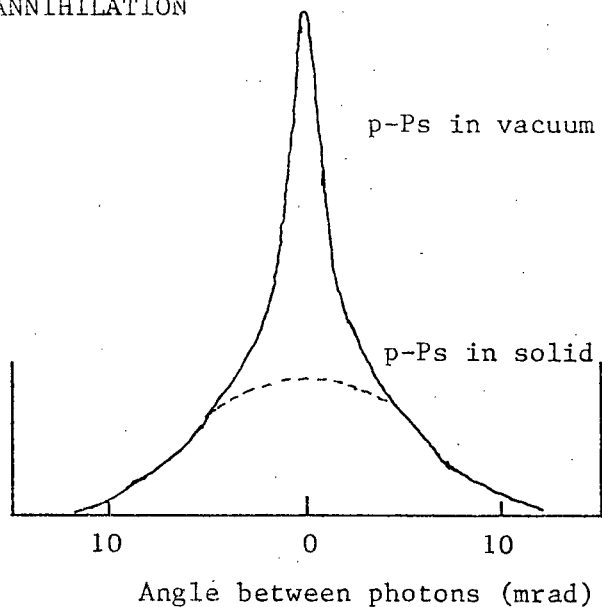
- 10a -  
POSITRONIUM ANNIHILATION

Parapositronium ( $^1S_0$ )

two quantum annihilation

$\tau_p \sim 0.12$  nsec

Angular correlation



Orthopositronium ( $^3S_1$ )

three quantum annihilation

$\tau_o \sim 140$  nsec

Gamma energy spectrum

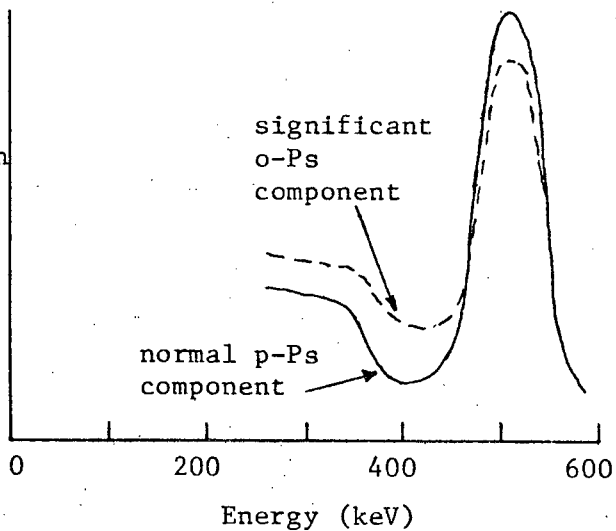


FIGURE 1

By starting a clock with the 1.28 MeV signal and stopping it with the detection of a gamma of 511 keV or less, one can determine the lifetime of the positron. Up to three medium-dependent lifetimes have been observed (Paulin and Ambrosino, 1968) in powdered insulators, corresponding to the different annihilation processes previously mentioned. The strength of the lifetime component due to pickoff of the positron in o-Ps is found to decrease as particle size is decreased, which can be explained in terms of the diffusion of o-Ps into the void between particles. A diffusion model, assuming uniform positronium thermalization in spherical powder particles followed by a random walk, was used to describe the data. The assumption of ejection of the atom into the vacuum at the particle surface was included. A fit of the pickoff component strength as a function of particle radius yielded the diffusion constant  $D$  for positronium in each of  $\text{SiO}_2$ ,  $\text{Al}_2\text{O}_3$ , and  $\text{MgO}$ .

### 3. Gamma spectrum analysis

While p-Ps annihilation leads to two gamma rays of 511 keV each, o-Ps must decay to three gammas (or at least an odd number greater than one) whose energy spectrum is continuous up to a maximum of 511 keV. By careful comparison of two spectra taken under identical conditions (except for those designed to enhance the three gamma process) one can discern a filling in of the valley region between the usual 511 keV peak and its Compton scattering edge at about 341 keV. The 511 keV peak is correspondingly reduced. This is observable in spectra from positrons injected into powders held in air and in vacuum, since three gamma annihilation is quenched in the presence of oxygen molecules due to spin exchange.

### C. Testing the Powder Samples

In order to assess the suitability of a particular sample of powder, the method of spectral analysis was used. Although quantitative interpretation is difficult with this technique, a difference in the particle size affects the fraction of positrons annihilating as o-Ps, which is in agreement with the model of positronium diffusion.

#### 1. Experimental design

The apparatus used for the positron segment of the experiment consisted of a four inch diameter by three inch cylindrical NaI(Tl) crystal mounted on an RCA XP1140 photomultiplier tube with its associated electronics, a pre-amplifier and pulse shaping amplifier, and a Victoreen PIP 400 multichannel analyzer for pulse height analysis. A  $^{22}\text{Na}$  source was deposited on a thin flat aluminum disk which could be submerged in a powder sample and held at a pressure of  $10^{-6}$  Torr by a diffusion pumping system. The source and powder were enclosed by glass in order to make the powder visible while pumping on it, as it had a tendency to "boil" into the vacuum pump.

#### 2. Data analysis

Approximately 20 runs of about 30 minutes each were made on various powder samples, both in air and in vacuum. The data were analyzed in the following way: contents of each of four sets (valley (V), annihilation peak (A), background (B), and prompt peak (P) ) of five channels apiece were separately totalled (see Fig. 2). The background due to the 1.28 MeV Compton scattered events (B) was subtracted from both the valley channels and the annihilation peak. These values were then normalized to the prompt

# POSITRONIUM ANNIHILATION IN QUARTZ POWDER

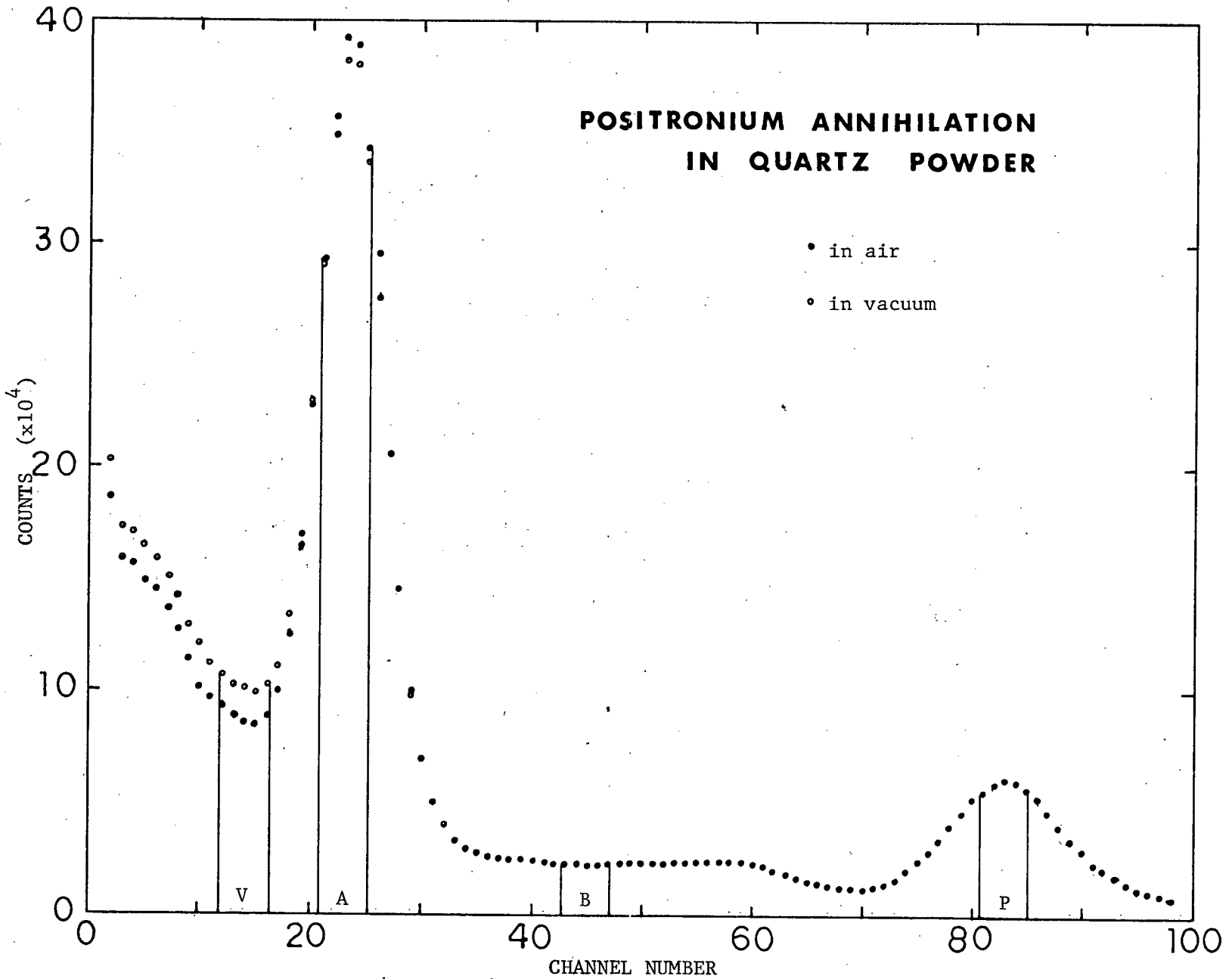


FIGURE 2

1.28 MeV peak and comparison was made between runs in air and in vacuum (as well as a run in vacuum baked-out at 200 C). The results are tabulated in Table IV. It should be emphasized that the figure "per cent effect" is not to be construed as a measure of the amount of triplet positronium in vacuo, but is for purposes of comparison between samples only. This figure is derived from the reduction in the strength of the annihilation peak, since the valley region is much more prone to error from background and increased efficiency at the lower energies. Obviously, the three gamma component can grow only at the expense of the two gamma 511 keV peak.

### 3. Results

As expected, the per-cent effect is largest for the powder of smallest grain size used, the 70 A diameter silica (Cab-O-Sil EH5) sample. It was smallest for a sample of larger, low-purity (~96%) magnesium oxide granules, which is in agreement with other experiments using MgO.

We have placed emphasis on the study of silica powders for two reasons: firstly, very fine, pure SiO<sub>2</sub> powder samples are commercially available at no cost; secondly, the behavior of muons and muonium in fused quartz is well established (Miyasishcheva et al, 1968, and Gurevich et al, 1971) and such behavior is a probable condition for the observation of muonium in vacuum. This will be clarified in the chapters on the experiment at TRIUMF.

POWDER MATERIAL	SIZE	AIR $\frac{V-B}{P}$	AIR $\frac{A-B}{P}$	VACUUM $\frac{V-B}{P}$	VACUUM $\frac{A-B}{P}$	PER CENT EFFECT
SiO <sub>2</sub> (Aerosil)		1.154±.003	5.700±.012	1.297±.004	5.498±.011	3.5±0.4
SiO <sub>2</sub> (Aerosil) baked out		1.154±.003	5.700±.012	1.318±.003	5.480±.009	3.9±0.4
SiO <sub>2</sub> (Cab-O-Sil)	70 A	1.153±.003	5.578±.011	1.349±.004	5.302±.011	4.9±0.4
SiO <sub>2</sub> (Cab-O-Sil)	140 A	1.113±.003	5.617±.010	1.285±.004	5.434±.011	3.3±0.4
MgO (impure)		1.116±.003	5.503±.009	1.375±.003	5.422±.010	1.5±0.4

TABLE IV. POSITRONIUM EXPERIMENTAL RESULTS

#### IV. The TRIUMF Experiment

The study of muonium and its behavior in a powdered insulator target is similar to that of positronium in that one can trace the life history of the  $F = 1$  state. There the similarity ends, for the muonium atom produces no annihilation quanta. One instead observes transitions among the  $F = 1$  substates of the atom, in the form of the polarization of the muons in these substates. Transitions involving the  $F = 0$  state occur at a frequency too high to be observed. The time dependence of the polarization provides information on the environment of muonium, which is the basic idea of MSR. The TRIUMF installation provides beams of highly polarized positive muons, a prerequisite for an MSR (or  $\mu^+$ SR) experiment.

## A. The Source of Muons

### 1. General

The dominant mode of positive pion decay, with lifetime  $\tau \sim 2.6 \times 10^{-8}$  sec is:  $\pi^+ \rightarrow \mu^+ + \nu_{\mu}$ . The resulting muons can be collected to form a beam.

The pions are in turn produced by irradiation of a target with an intense, well-focussed proton beam. TRIUMF produces such a beam at 500 MeV, utilizing for pion production a reaction such as:  ${}^9_4\text{Be} (p, \pi^+) {}^{10}_4\text{Be}$ .

The conventional mode of beamline operation is to collect muons from in-flight pion decay. The decay can take place either near the production target, producing so-called cloud muons, or in the beam line, in which case either the forward or backward (with respect to beam direction) decay muons are selected by subsequent momentum analysis. Each process leads to a different set of beam properties such as flux, momentum, profile, and contamination (proton, pion, and positron).

### 2. The TRIUMF M9 channel

The M9 channel is a multipurpose low energy and stopping pion or muon beam line, designed and built by the University of Victoria contingent at TRIUMF. It consists, for our purposes, of seven magnetic elements, which focus particles, emitted from the production target in a solid angle of  $\sim 60$  milliradians at  $135^\circ$  to the proton beam, onto the target of interest. Two of the elements are  $45^\circ$  bending dipoles, the remaining five being ten inch quadrupole lenses, arranged symmetrically about the midpoint as shown in Fig. 3. Particles produced in the proton target are focussed to a beam spot which is essentially a  $45^\circ$  plane projection of the target.

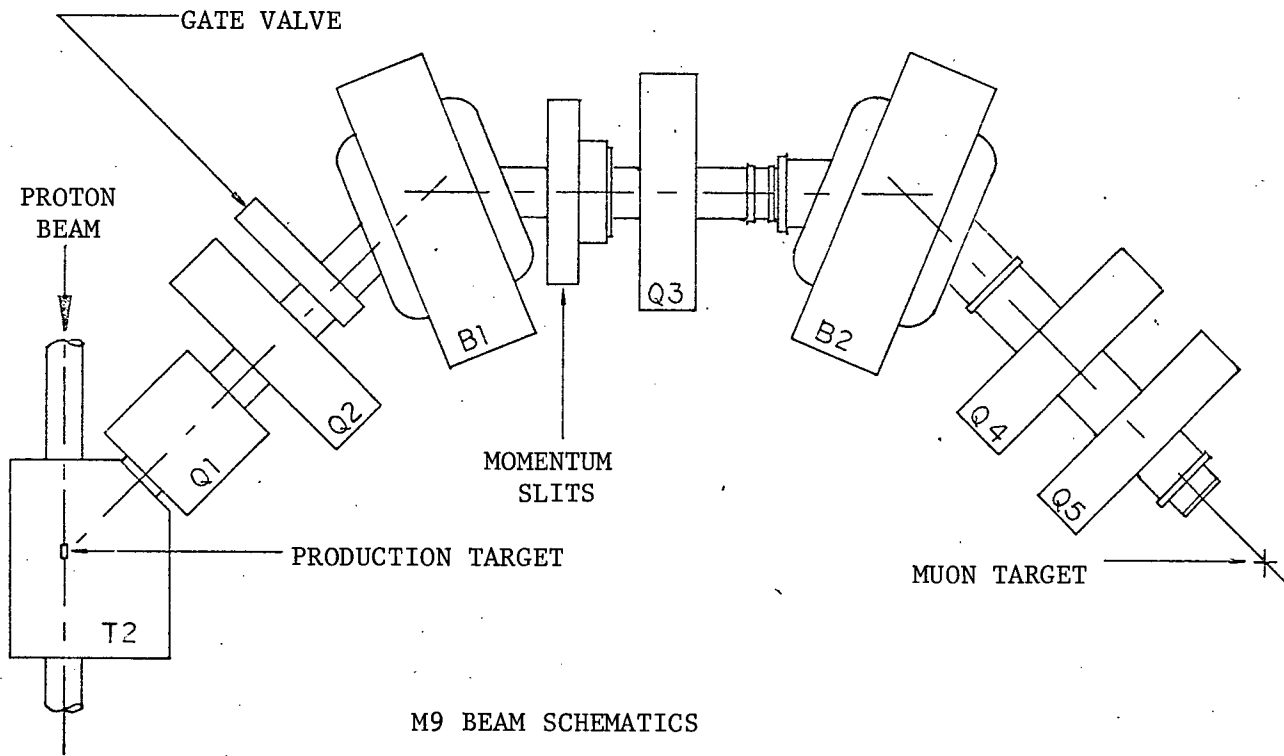


FIGURE 3

M9 BEAM SCHEMATICS

### 3. Surface muons

Conventional modes of muon production are not compatible with good focussing characteristics, since the muons do not come directly from the proton target. There are, however, a large number of pions that decay at rest close to the skin of the target, producing muons which can be sharply focussed by a beam line (Pifer et al, 1976).

A beam of these muons has certain other properties which can be advantageous. The polarization is high ( $> 95\%$ ), the momentum is well defined (a maximum of 29 MeV/c), and the range is short ( $148 \text{ mg/cm}^2 \text{ CH}_2$ ), making it ideal for MSR studies in low density materials such as gases and powders.

One would expect protons, pions, and positrons of 29 MeV/c to contaminate such a beam, but only the positrons are present at the muon target. The protons do not pass through the thin (2 mil mylar) window at the beam pipe exit. Only about 0.3% of the pions remain due to decay during a time of flight of about six mean lifetimes, and these have a range of the order of one-third that of the muons. The positrons, on the other hand, have a rather ill-defined range  $\sim 100$  times greater than the muons, and do not stop in a low density target.

### 4. Detection of low energy muons

The short muon range necessitates the use of a very thin counter system, since one must identify the time at which the muon enters the target by passing it through a scintillator.

The system used consisted of a single four inch square sheet of 15 mil ( $40 \text{ mg/cm}^2$ ) NE102 plastic scintillator. Light collection was facilitated

by a wedge shaped aluminized mylar sheath supported in a lucite frame which reflected light from the scintillator towards the wider end of the wedge, where it was guided via the usual lucite light guides to an RCA8575 photomultiplier. A second sheath of 0.3 mil aluminum foil provided a light tight wrapping. Due to much lower energy deposition by 29 MeV/c electrons in comparison with muons, the photomultiplier high voltage and signal discrimination levels can be adjusted so as to provide a clean muon trigger with high efficiency and good time resolution.

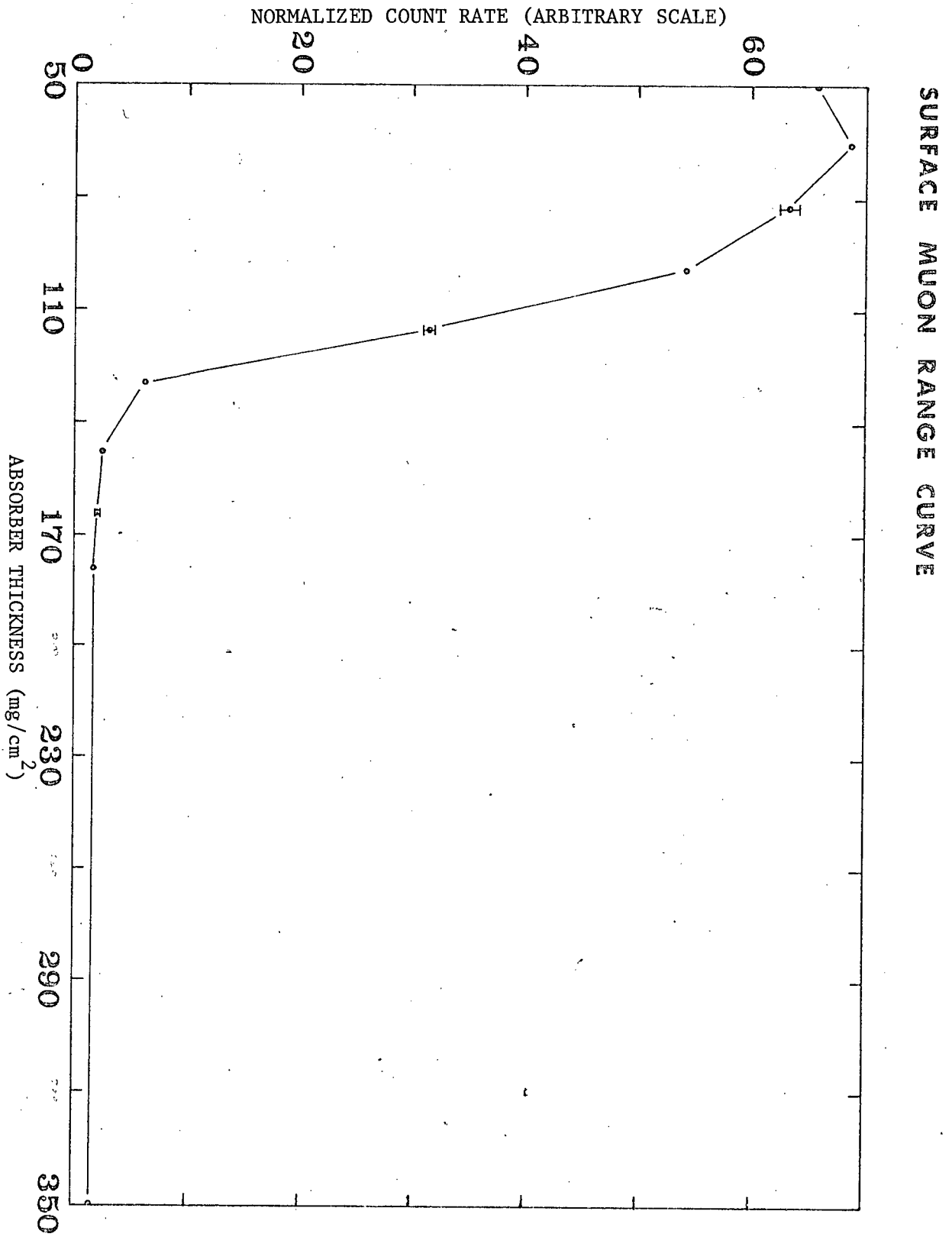
#### 5. Tuning for surface muons

The M9 channel was initially adjusted for surface muons by scaling the bending magnet currents down by the momentum ratio, since it was known that hysteresis effects were small. With all quadrupoles off, the counting rate in the muon detector was maximized by fine adjustment of the bending magnets. The quadrupoles were then turned on to the approximate (scaled) settings, and fine adjustments were made by an iterative process, again by maximizing the rate. Fluxes as high as  $5 \times 10^4$  positive muons per second were achieved in the four inch square scintillator, at one microampere proton current.

In order to identify the muons unambiguously, an integral range curve was measured by scaling the muon counter as a function of thickness of mylar absorber at the beam pipe exit. The curve is shown in Fig. 4.

A muon precession curve in copper proved that the particles were muons rather than pions. Beam profiles were measured in a subsequent experiment, and showed the muon spot to be roughly elliptical in shape, three inches wide by two inches high.

FIGURE 4



## B. The MSR Time Spectrum

The MSR technique is based on two intrinsic qualities of the muon, its asymmetric decay and its magnetic moment. Due to maximal parity violation in the process  $\mu^+ \rightarrow e^+ + \nu_e + \bar{\nu}_\mu$  ( $E_{\max} = 52.8$  MeV), the positrons are emitted with an angular distribution  $1 + a \cos\theta$ , where  $\theta$  is the angle between the positron direction of flight and the  $\mu^+$  spin (in the  $\mu^+$  rest frame) at the instant of decay. The asymmetry parameter  $a$  is a function of the decay positron energy  $E$  (Fig. 5):

$$a = \frac{2w - 1}{3 - 2w}, \quad w = E/52.8 \text{ MeV}.$$

This asymmetric behavior provides a method of observing the rotations of the spin magnetic moments of a time ensemble of muons in a transverse magnetic field. (Fig. 6)

### 1. Rotation

In contrast with  $\mu^+$ SR, where the rotation of free muons is observed, MSR is the rotation (and relaxation) of the  $^3S_1$  state ( $F_z = 1$ ) of the muonium atom. Here the muon spin is coupled to that of the electron by the hyperfine interaction. The magnetic moment of the system gives rise to Larmor precession in low magnetic fields, at the frequency  $\omega_M$ , where:

$$\omega_M = \frac{1}{2}(\omega_\mu + \omega_e) \sim -103\omega_\mu$$

The factor of one-half is due to the precession of a spin one state, rather than spin one-half, since the individual magnetic moments depend on the charge-to-mass ratio,  $\omega_e \sim -207 \omega_\mu$ , and the sense of rotation for muonium is opposite to that of a free muon. Numerically,  $|\omega_M/B| \sim 2\pi:1.394$  MHz/gauss, for  $B \lesssim 50$  gauss. In higher fields, Zeeman couplings cause a split in

POSITRON ENERGY SPECTRUM AND ASYMMETRY PARAMETER

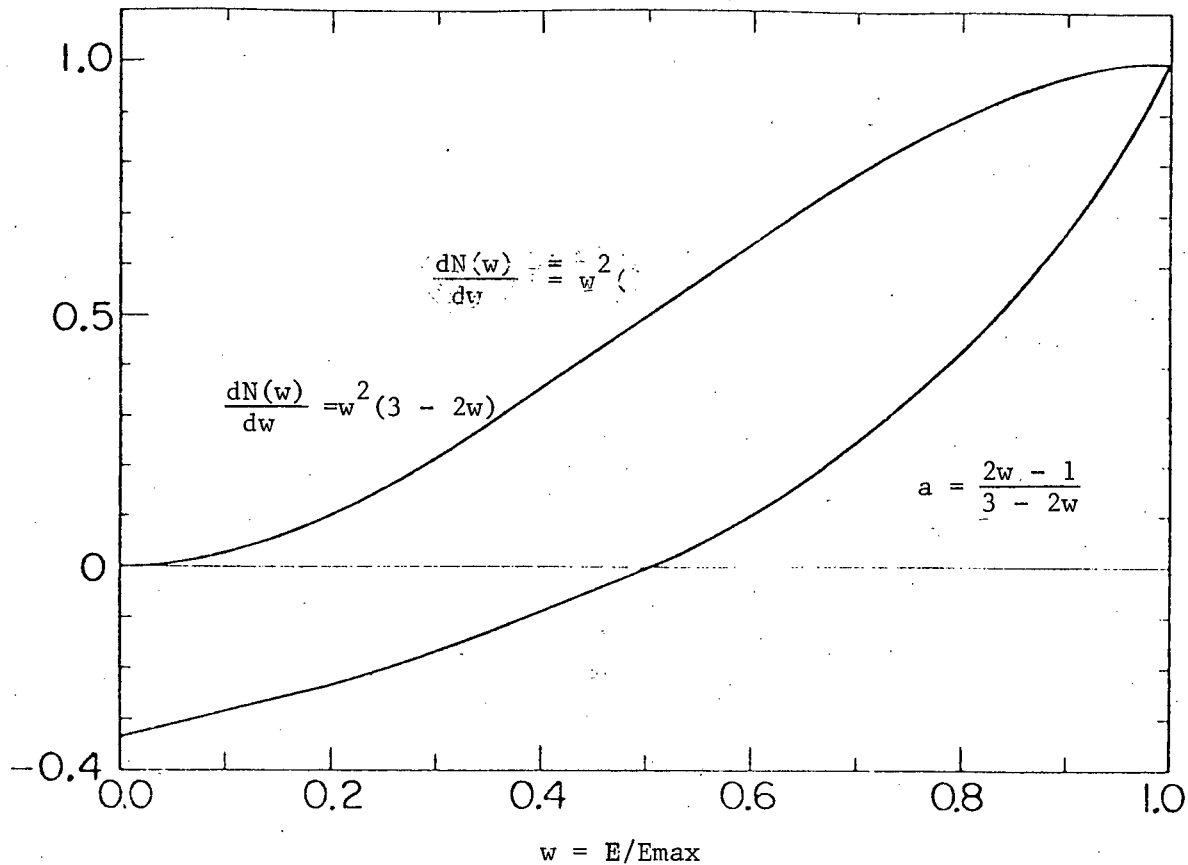
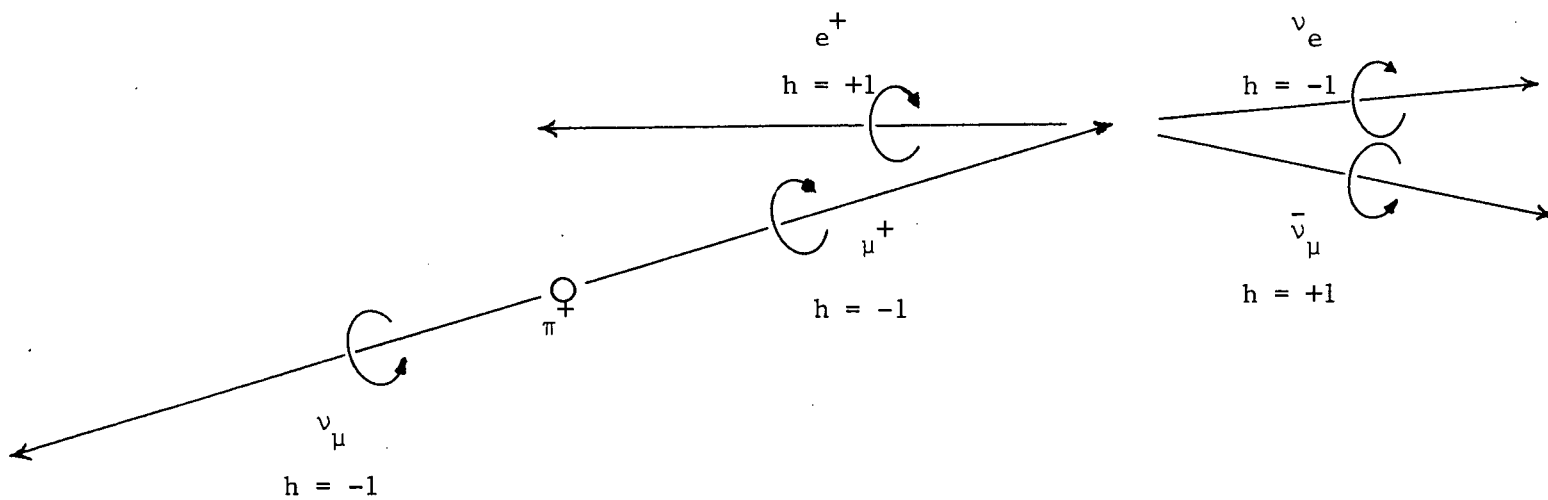


FIGURE 5

FIGURE 6



HELICITIES IN  $\pi^+ \rightarrow \mu^+ \rightarrow e^+$  DECAY

frequency (Gurevich et al, 1971, and Brewer et al, 1974) and a beat phenomenon is observed.

## 2. Relaxation

The average of the muon decay asymmetry 'a' over all possible positron energies is one-third, but in practice one does not detect all positrons with the same efficiency. Moreover, all muons do not form triplet ( $F_z = 1$ ) muonium and the beam may not be 100% polarized, which leads to a reduction in the observed asymmetry. Therefore, we do not measure 'a' directly, but a more subtle quantity  $A_0$ , the experimental asymmetry at the time the triplet muonium atoms form in the transverse field. It is the time evolution of the experimental asymmetry A that has spawned another meaning for the MSR acronym, Muonium Spin Relaxation; the relaxation of the spin due to depolarizing effects of various kinds provides valuable information on the environment of the Mu atom. Applied field inhomogeneity, random local fields, and chemical reactions are sources of relaxation. Collisions with paramagnetic molecules such as  $O_2$  lead to an exponential decay of the asymmetry at a rate proportional to the probability of collisions, that is, the gas pressure. This result can be summarized:  $A(t) = A_0 \exp(-t/T_2)$ . The quantity  $T_2$  is called the relaxation time.

## 3. Spectral form

Overall, the form of the muonium decay time spectrum is:

$$N(t) = N_0 \left\{ e^{-t/\tau} \left[ 1 + A_0 e^{-t/T_2} \cos(\omega_M t + \phi) \right] + B \right\}$$

The parameter  $\tau = 2.2 \mu\text{sec}$  is the muon lifetime. The phase  $\phi$  depends

on positron telescope geometry and the difference between the time of formation of muonium and the experimental  $t = 0$  (usually small).  $N_0$  is a normalization factor while  $B$  takes into account the background, assumed to be constant.<sup>†</sup>

#### 4. Typical muonium and muon spectra

A typical muonium spin rotation spectrum obtained using a fused quartz precession target is displayed in Fig. 7. In Fig. 8, a plot of the asymmetry as a function of time is shown for muons in a liquid carbon tetrachloride target (obtained by folding out the background and exponential decay). Both of these were obtained in a conventional muon beam. Fig. 9 shows the precession of surface muons at TRIUMF in a copper target. Both muon spectra were taken with the applied transverse field of 75 gauss, while the muonium spectrum was at 4.2 gauss.

<sup>†</sup> With a large free muon component, one should assume a linear time dependence for  $B$  (Fleming et al, 1976).

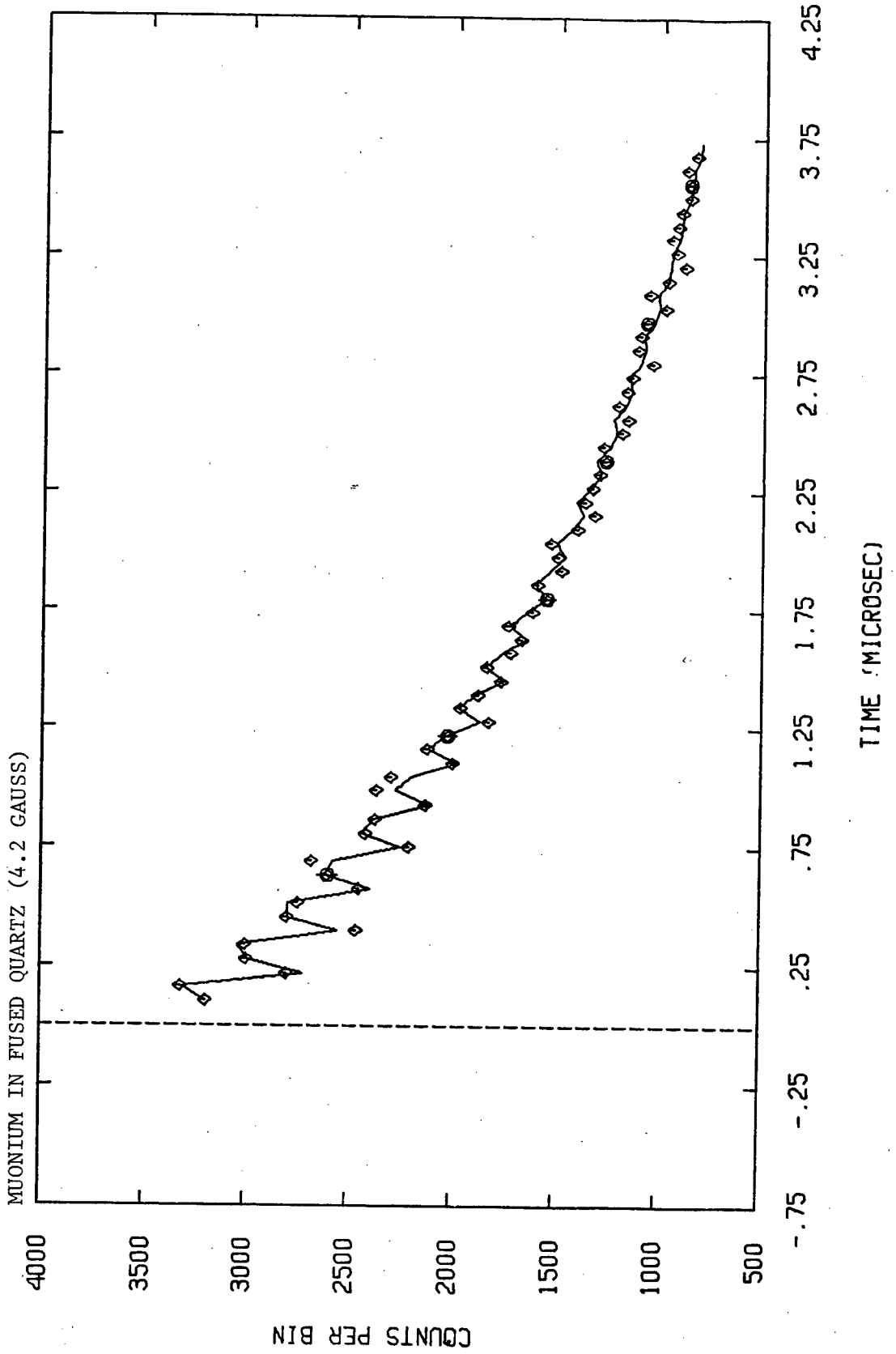
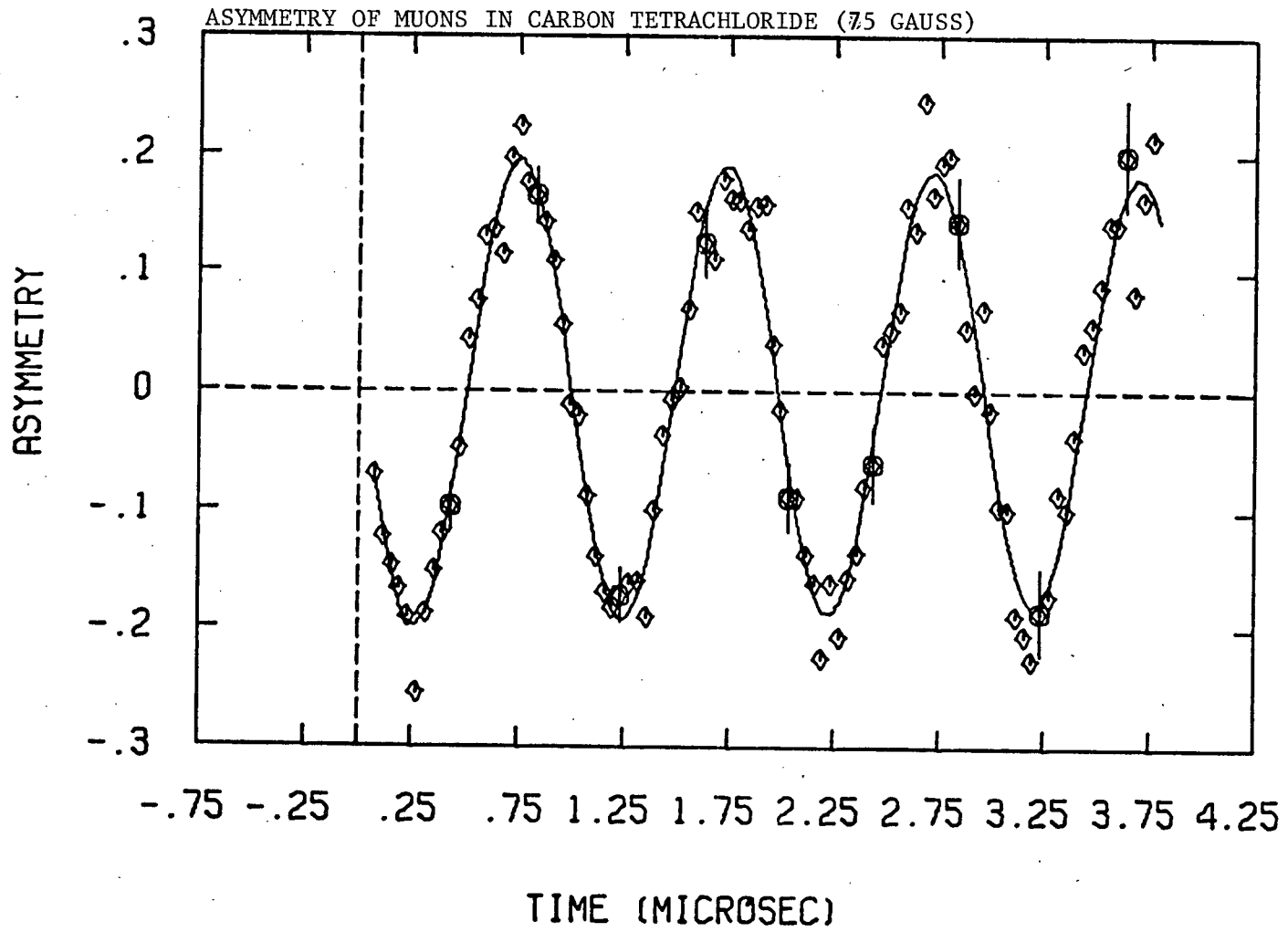


FIGURE 7

FIGURE 8



MUON PRECESSION IN COPPER (75 GAUSS)

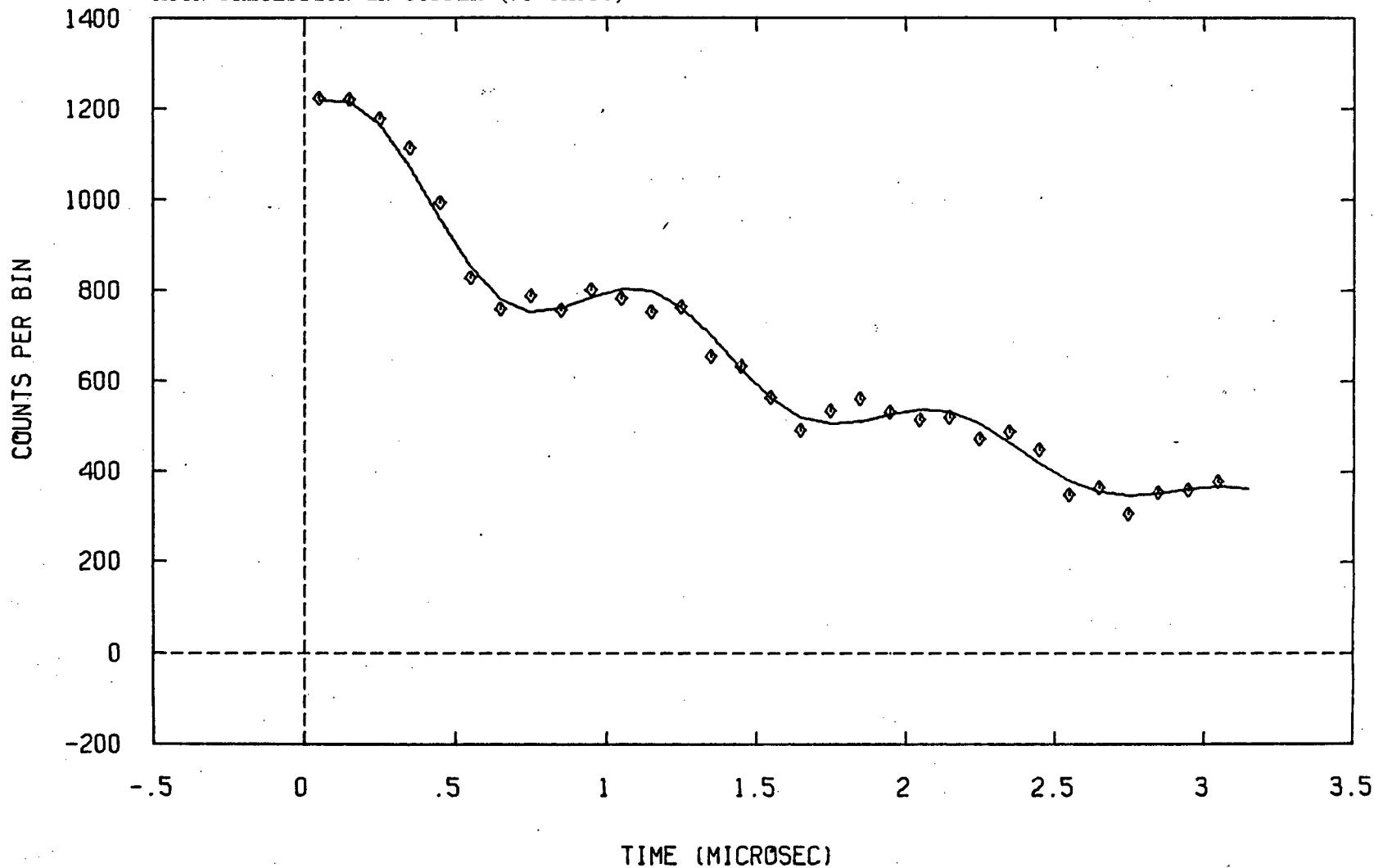


FIGURE 9

## C. Apparatus

### 1. Precession cart

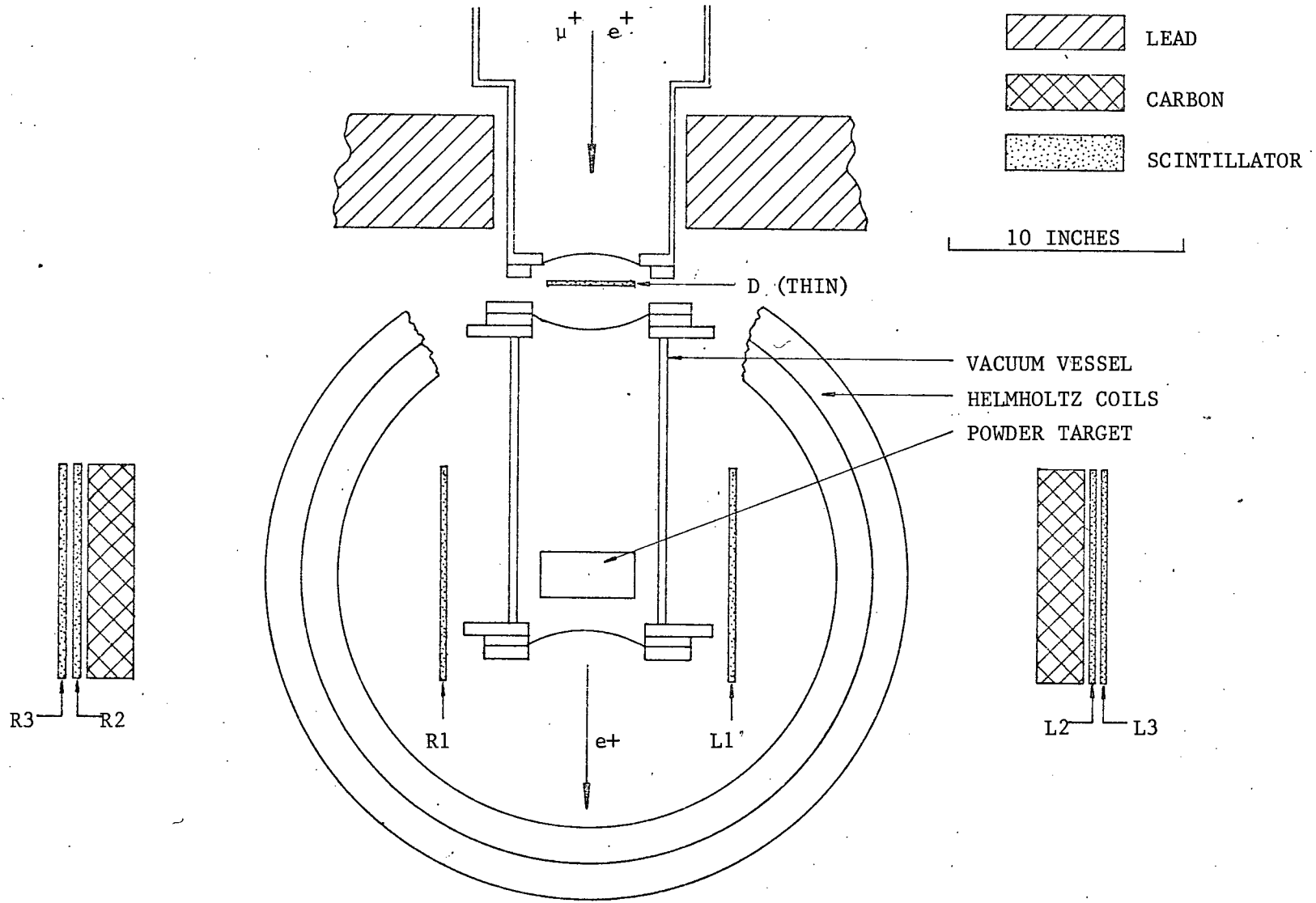
The technique of MSR was applied to search for the formation and diffusion of muonium in silica powders. The main components of the apparatus as shown in Fig. 10 are; the thin defining counter, two positron telescopes, Helmholtz precession coils, and a target vacuum chamber with a diffusion pump and support assembly. The use of a wheeled precession cart makes the apparatus portable and the geometry reproducible.

The two positron telescopes view the muon stopping region in a direction perpendicular to both the beam direction and the applied transverse field. Each telescope consists of three 8" x 16" x  $\frac{1}{4}$ " plastic counters, one near the target and two farther away, separated by 2" of graphite degrader to reduce scattered positron background and discriminate against low energy (and hence negative asymmetry) decay positrons. All counters use RCA 8575R photomultipliers. The telescopes were designed and built by the University of Arizona group at Lawrence Berkeley Laboratory, as were the precession coils, and have been modified for use at TRIUMF.

The coils themselves are dual Helmholtz type, the extra set of coils enhancing the field uniformity. A deviation of less than  $\pm 0.1\%$  over a volume of 400 cubic centimetres minimizes depolarization due to field inhomogeneity. The maximum field available is over 75 gauss, sufficient for both muonium and muon precession studies.

The vacuum chamber in which the target is supported consisted of a glass cylinder 6 inches in diameter and  $15\frac{1}{2}$  inches long, with brass and aluminum flanges on each end supporting mylar windows. The upstream (5 mil)

FIGURE 10



PRECESSION APPARATUS

window allowed muons (and positrons) into the target while the downstream (10 mil) one allowed parasitic use of the positrons behind our apparatus. Our entire experiment did not present enough mass to the beam to scatter positrons appreciably.

Two ports on the upper and lower sides of the cylinder provided, respectively, a line to the vacuum pump and a connection through two closely spaced needle valves to an oxygen supply.

The powder itself was put in a wire-supported mylar vessel with a 0.25 mil aluminized mylar face to allow muons into the target. It was open at the top to permit the interstices to be evacuated. This was done by means of a diffusion pump with a cold trap. Pressure was measured with a UBC-NP-12 type ionization gauge for high vacuum and a Pirani gauge for lower vacuum.

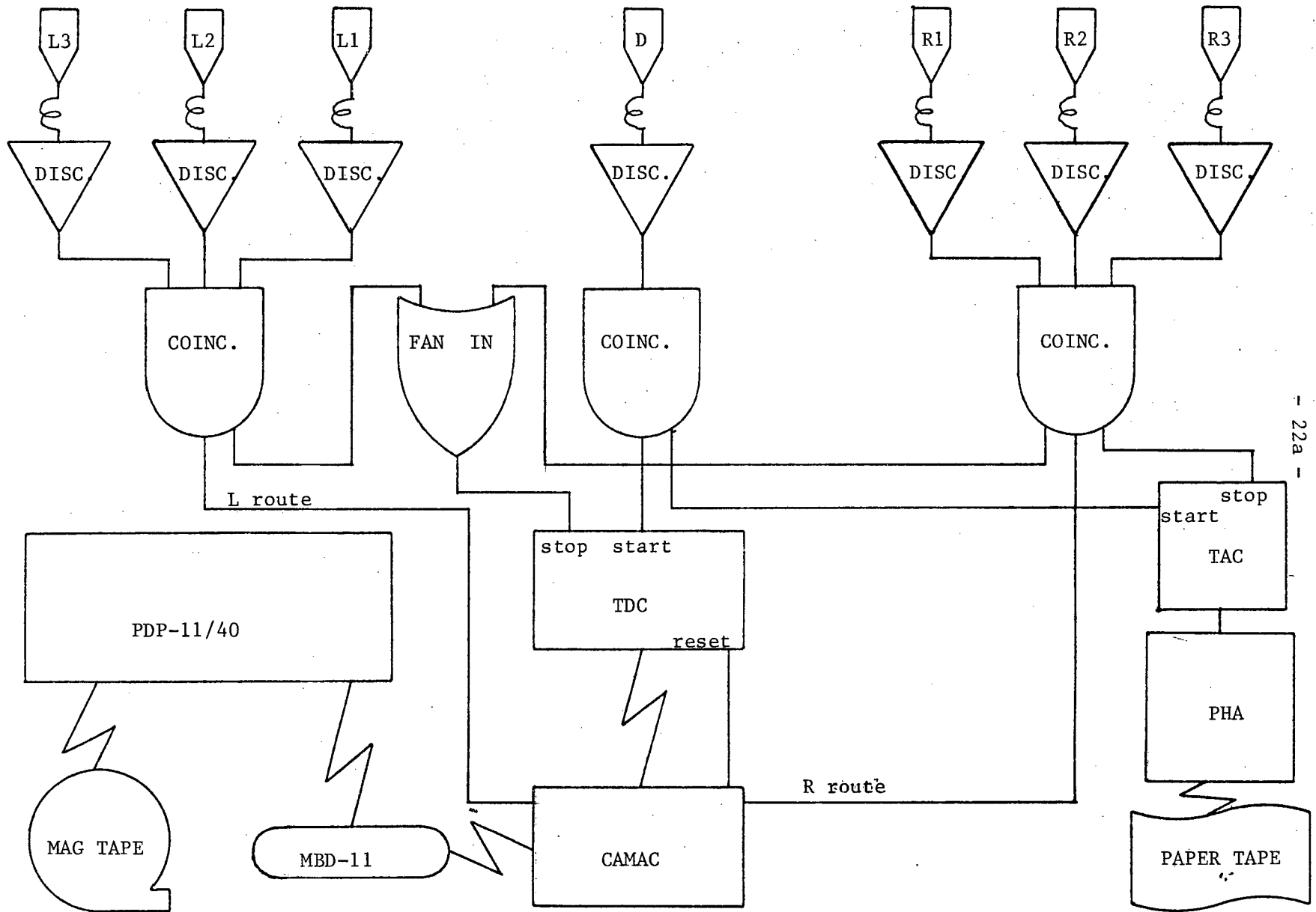
## 2. Electronics and data collection

Signals from the photomultiplier bases in the experimental area were fed via 100 foot cables to the electronics configuration shown in Fig. 11. The stopping muon logic is virtually nonexistent in this configuration for two reasons. First, the clean, noiseless signal from the muon counter eliminates need for a coincidence to define the incoming particle. Secondly, the inefficiency of electron counting in the thin plastic makes an electron veto counter unnecessary.

No muons have sufficient energy to pass completely through the target vessel.

Start and stop signals from one telescope were fed to an Ortéc 437A time-to-amplitude converter coupled to a Tracor-Northern pulse height analyzer

FIGURE 11



and punched on paper tape. Time histograms from stop signals in both telescopes were accumulated simultaneously with a PDP-11/40 using an EG&GTDC100 time digitizer connected via CAMAC and an MBD-11 programmable branch driver. These histograms were recorded on magnetic tape.

#### D. Muonium in Silica Powder

##### 1. Quenching technique

The vacuum system on the precession cart was assembled the day before the run at TRIUMF. A sample of 70 Å diameter silica powder identical to that used in the most successful positronium study was inserted. The system was pumped at  $10^{-6}$  Torr for four hours to remove impurities (eg. hydroxyl groups, siloxane, water) from the granule surfaces. It was kept overnight at  $\sim 2 \times 10^{-2}$  Torr until an hour before the first run, when diffusion pumping was resumed. The pressure for that run was  $\sim 10^{-6}$  Torr. The transverse magnetic field applied in this and subsequent runs was 2.5 gauss.

Oxygen was then introduced, at a pressure of  $0.4 \pm 0.05$  Torr, for the second run, in order to check whether depolarization (or "quenching") would take place. The high vacuum run was repeated with better statistics, followed by two runs at  $0.05 \pm 0.005$  Torr and  $0.15 \pm 0.02$  Torr oxygen pressure. Another high vacuum run, a run with a low pressure xenon atmosphere, and a run at high vacuum with a mylar shield on the inside surface of the glass vessel, followed the initial runs.

If muons form muonium in a powdered sample as they are known to do in bulk quartz<sup>†</sup>, precession at the muonium frequency will be apparent. If

they do not reach the powder surface, the addition of a small component of oxygen to the target will have little effect. If, however, there is fast diffusion to the surface, the paramagnetic oxygen molecules will depolarize the muonium and quench the precession at that frequency. Moreover, if the powder acts as an inert moderator (essentially a dense inert gas) the dependence of the relaxation rate,  $T_2^{-1}$ , on the oxygen partial pressure could be similar to the result from the gas chemistry of muonium (Garner et al, to be published).

The addition of xenon, on the other hand, should increase the muonium formation probability, since it is known that small admixtures of xenon in other inert gases enhances the muonium formation probability, with no depolarizing effect. To ensure that the glass walls of the vessel were not responsible for the muonium present, they were shielded with mylar shortly before the end of the shift.

## 2. Results

Analysis of the time histograms obtained was done off line on the IBM 370/168 at the UBC Computing Centre. The data were fitted to the form (5) by the routine VARMIT, and the results obtained are summarized in Table V. Plots of some of the data and the best fits are shown in Figures 12 - 15.

The plots show a clear trend in the relaxation of the precession signal as a function of oxygen pressure; depolarization is taking place.

† This was observed in a prior run at TRIUMF, and has been observed elsewhere (Miyasishcheva et al, 1968, and Gurevich et al, 1971).

RUN	EVENTS ( $10^3$ )	STANDARD DEVIATIONS	$A_o$	$T_2$ ( $\mu$ sec)	FIELD (gauss)	PRESSURE (Torr)	COMMENTS
1	34	-0.13	0.071(6)	9(6)	2.49	$10^{-6}$	Low statistics
2	132	-1.22	0.06(1)	0.3(1)	2.48	$0.4_0 O_2$	
3	77	+0.95	0.091(7)	8(5)	2.48	$10^{-6}$	
4	100	-0.39	0.060(3)	2.0(3)	2.48	$0.05 O_2$	
5	16	-0.21	0.09(2)	0.9(3)	2.58	$0.15 O_2$	Low statistics
6	112	-1.20	0.082(4)	6(2)	2.49	$10^{-6}$	
7	31	+0.26	0.19(2)	0.28(5)	2.56	$\sim 1$ Xenon	Probable $O_2$ contamination
8	23	+0.48	0.093(7)	12(4)	2.44	$10^{-6}$	Mylar shield used

TABLE V. MUONIUM EXPERIMENTAL RESULTS

MUONIUM IN SILICA POWDER AT  $10^{-6}$  TORR (2.5 GAUSS)

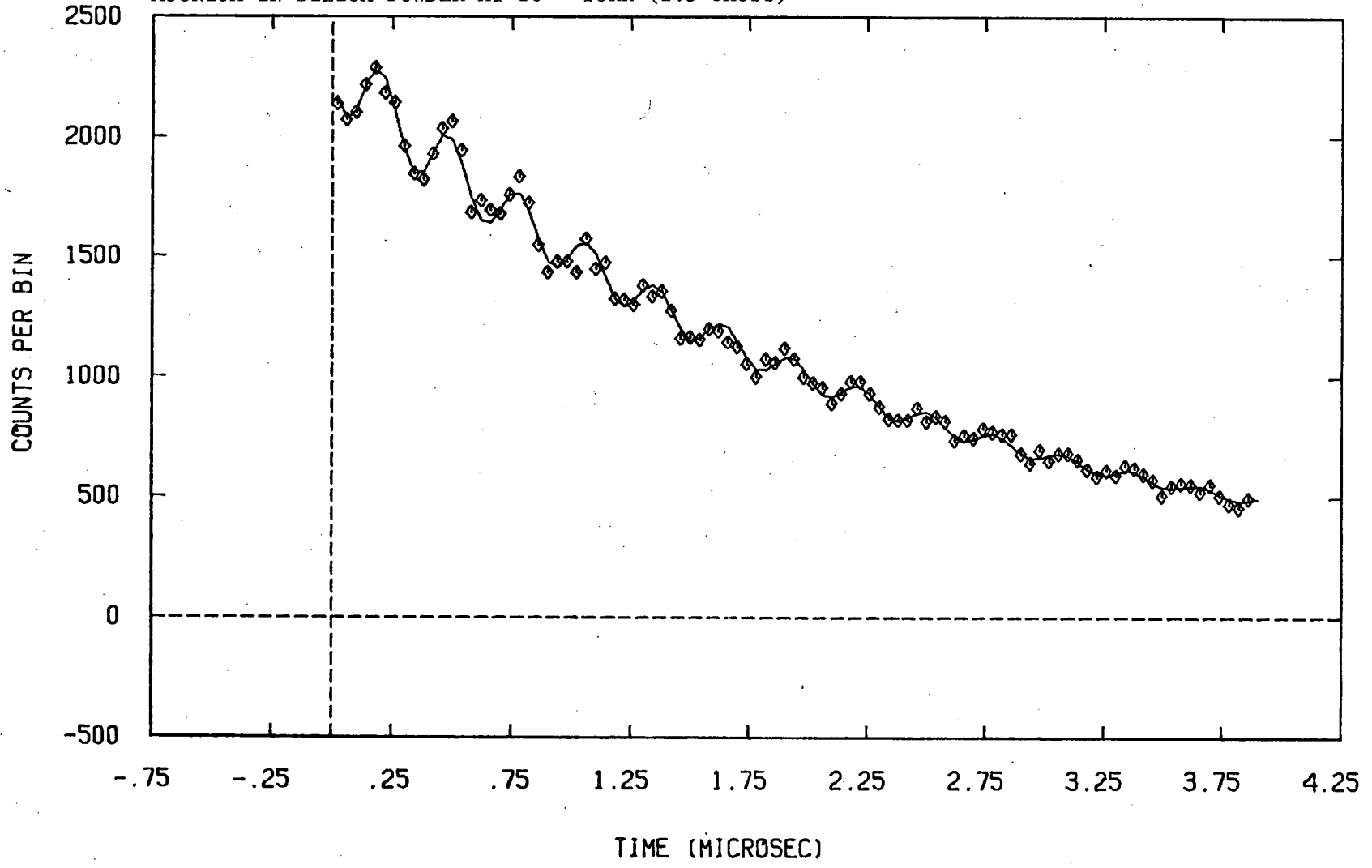


FIGURE 12

MUONIUM IN SILICA POWDER AT 0.05 TORR (2.5 GAUSS)

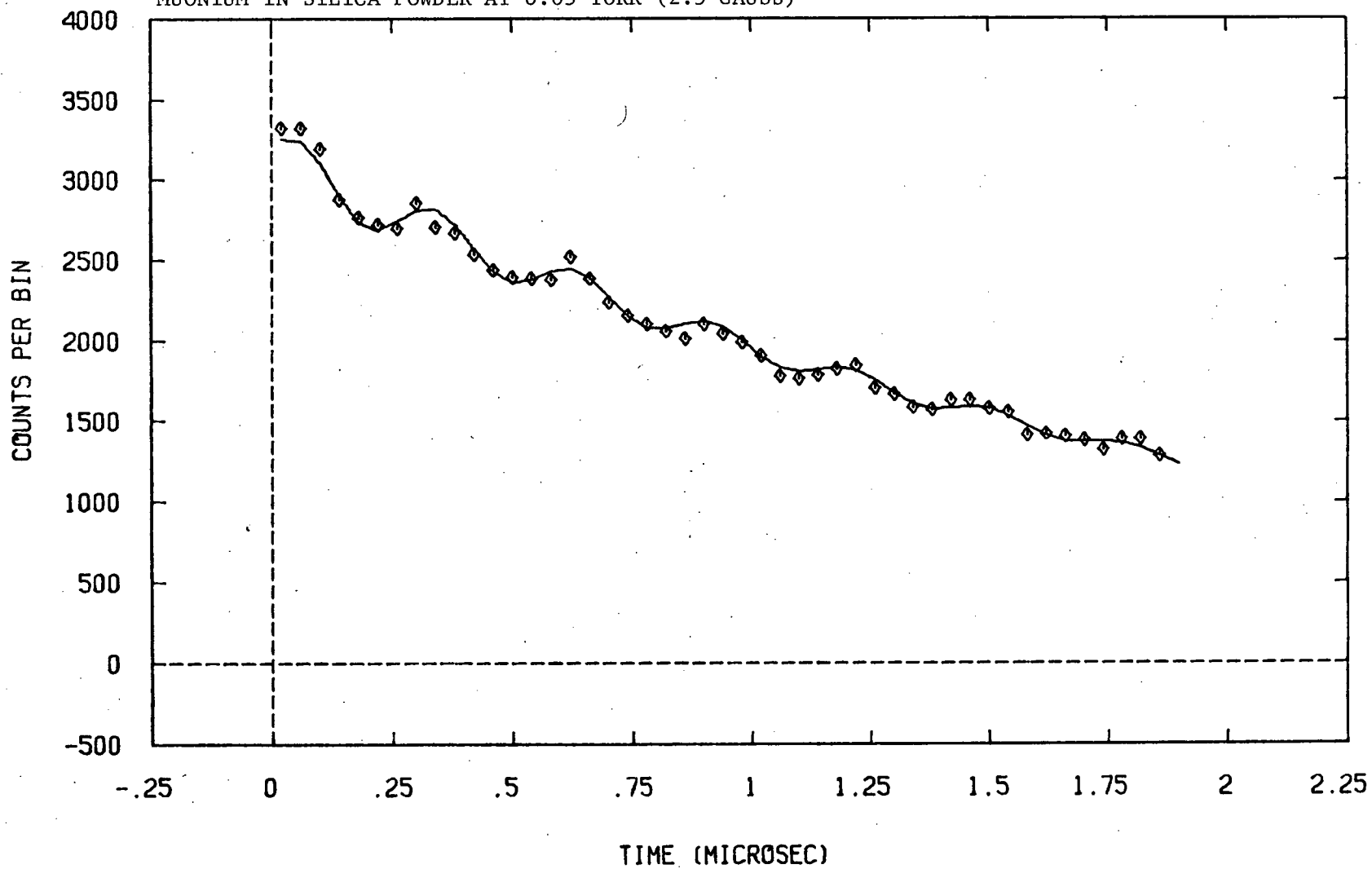
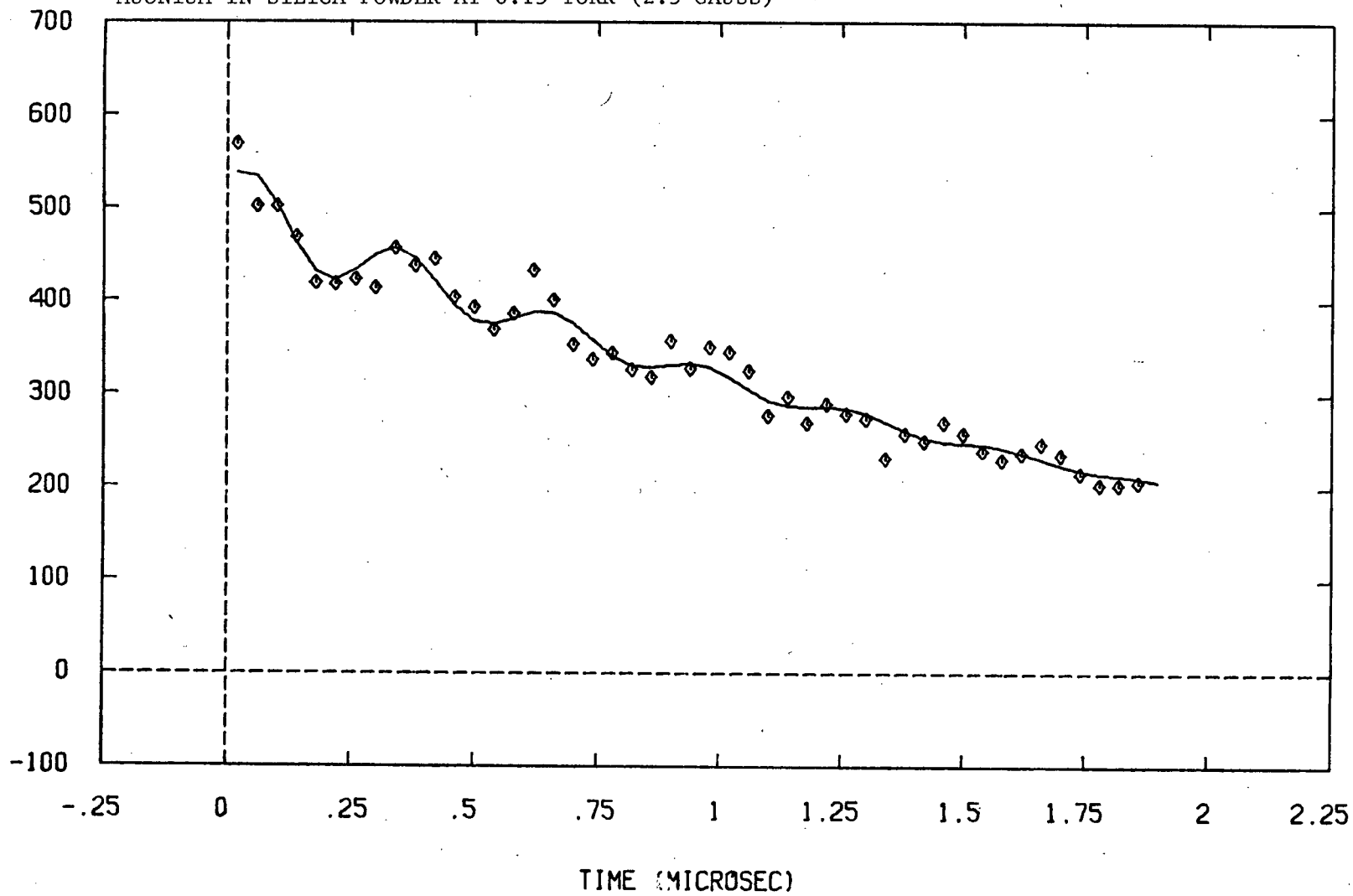


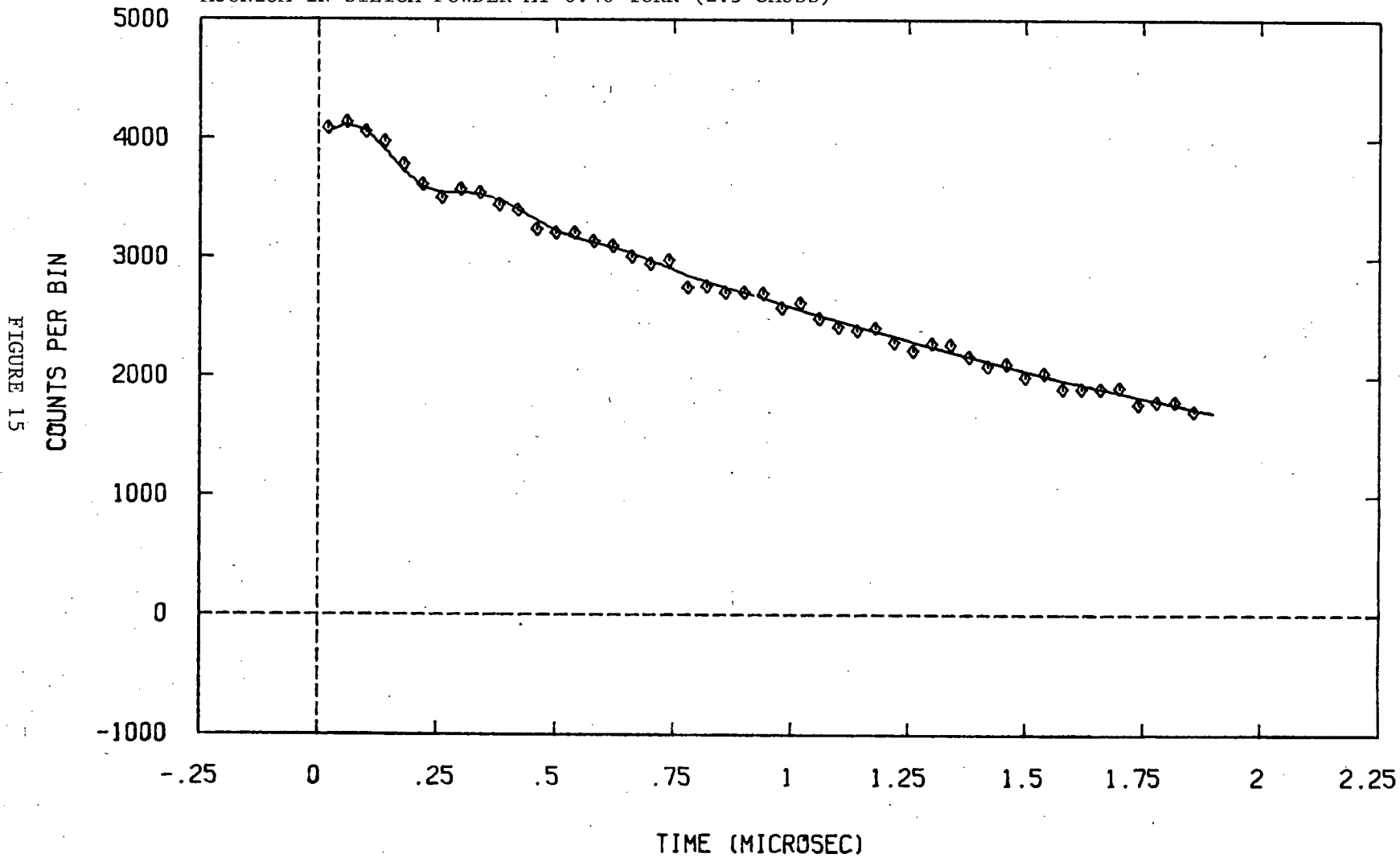
FIGURE 13

MUONIUM IN SILICA POWDER AT 0.15 TORR (2.5 GAUSS)

FIGURE 14  
COUNTS PER BIN



MUONIUM IN SILICA POWDER AT 0.40 TORR (2.5 GAUSS)



V. Evaluation; Diffusion of Muonium into a Vacuum

The presence of muonium depolarization when oxygen is added in small amounts to the target chamber constitutes evidence for the diffusion of the atom in the silica granules.

#### A. Qualitative Assessment

The extent of the diffusion in the powder is not well defined in our experiment. The argument can be made that a muonium atom would depolarize in the powder granule if it diffused to the surface and interacted there with adsorbed oxygen. Adsorption of oxygen certainly takes place on the powder surface, resulting in the formation of a siloxane group (Cabot Corporation, 1976) but there are several facts contradicting this as a depolarizing mechanism. The linear dependence of the relaxation rate,  $T_2^{-1}$ , on the oxygen pressure (Fig. 16) supports the contention that muonium is finding the void and depolarizing there. Secondly, adsorbed oxygen does not have the paramagnetic (depolarizing) character of the gaseous atom. Thirdly, the positronium results demonstrate that annihilation takes place in the vacuum, and muonium, being a neutral atom, should behave in a similar fashion at the solid-vacuum interface. In other words, if the atom gets to the surface, the potential barrier is such that it should escape to the void. It will remain there, since the thermal energy is small in comparison with typical barrier potentials at the surface of a solid.

#### B.

RELAXATION RATE AS A FUNCTION OF OXYGEN PRESSURE

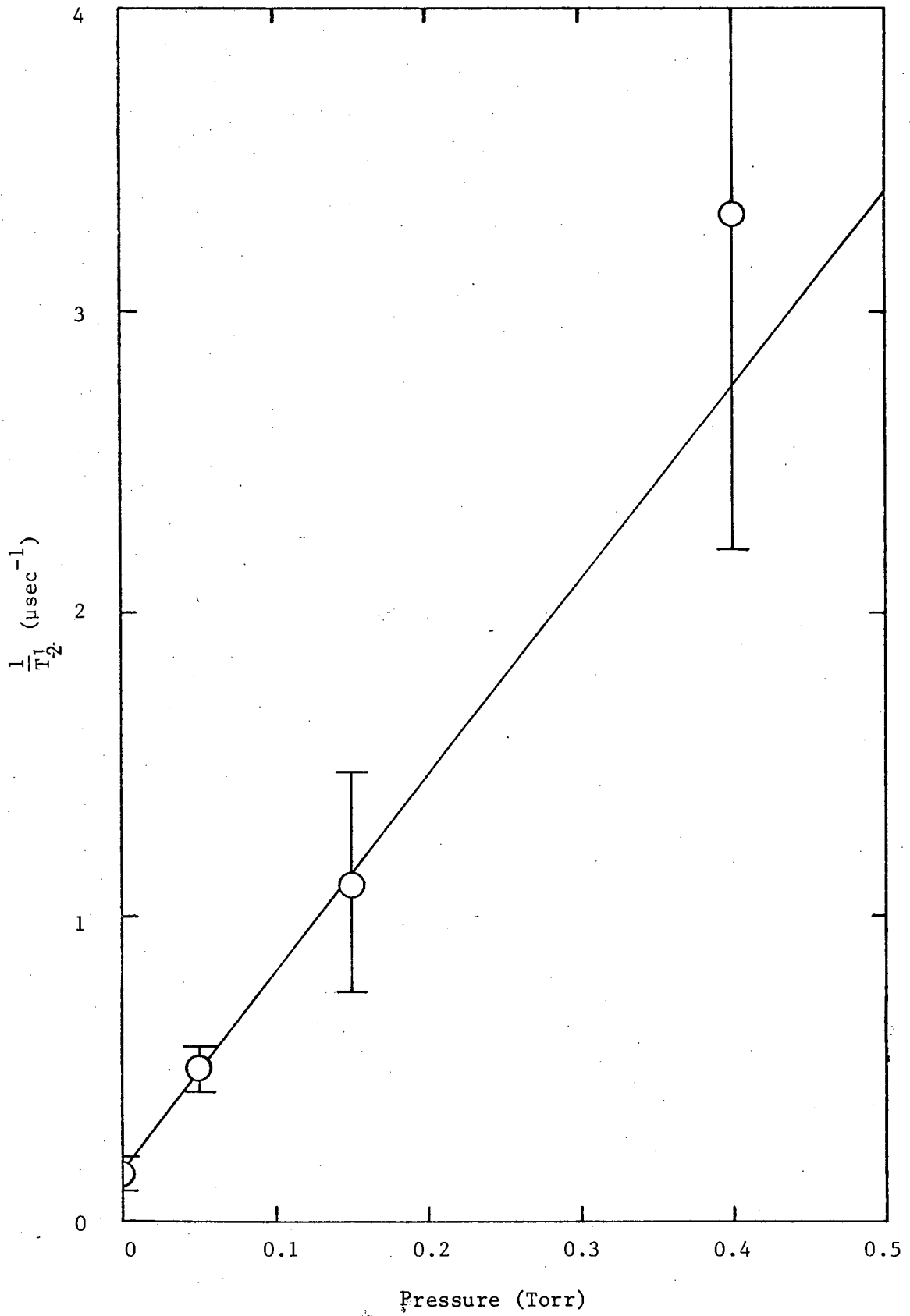


FIGURE 16

## B. Quantitative Consequences of the Muonium Asymmetry

Some idea of the amount of muonium present in vacuum can be extracted if one is prepared to make a few reasonable assumptions. From the evidence of fast diffusion just given, it is plausible that all the muonium formed eventually finds the void, since the mean lifetime ( $2.2 \mu\text{sec}$ ) is long compared to the relaxation time of  $0.3 \mu\text{sec}$ . However, in the powder target, the probability of muonium formation is not one, but is reduced. This probability can be estimated by analysis of the muonium asymmetry, which is  $\sim 0.08$  on the average for our experiment (excluding the Xenon run, where formation is enhanced due to the presence of a donor gas). With our experimental arrangement, the maximum observable asymmetry (ie., with no depolarization present) is of the order of 0.4 for a muon signal. This is reduced by one-half for muonium since in the atomic state, only the triplet precession is recorded. Therefore, roughly 40% of the muons injected decay as muonium in the particle interstices.

### C. Applications in Future Experiments

#### 1. Feasibility of an antimuonium experiment

With this information the possibility of attempting an antimuonium conversion experiment at TRIUMF can be critically examined. For one microampere of proton current on the production target, typical surface muon stop rates are of the order of  $4 \times 10^4$  per sec, of which  $\sim 1.6 \times 10^4$  decay as muonium in vacuum. If collisions with the powder particles have little effect on the degeneracy of the  $M-\bar{M}$  states, one can expect the conversion probability of  $2.5 \times 10^{-5}$  to hold in the absence of external fields, so that  $\sim 4$  conversions take place in one second. Experimentally, this is not prohibitively small.

There are two possible methods for detecting the conversion. The most sure is the observation of a fast electron from negative muon decay, which requires magnetic analysis to differentiate the electron from the vast positron background due to normal positive muon decays. Solid angle considerations imply the necessity of a rather large fancy device such as a spark chamber.

A somewhat easier approach is the search for muonic X-rays in the target material. The probability of breakup of antimuonium is high in dense materials, and should be high in the powder environment. Taking into account a 10% detector efficiency for, say, the silicon muonic  $K\alpha$  X-ray at 400 keV, and a solid angle of 5%, the overall probability of observing antimuonium in this way is  $\sim 0.5\%$ .

This gives an expected event rate for an experiment of this kind performed at TRIUMF of  $\sim 2 \times 10^{-3}$  per sec, or  $\sim 7$  events per hour. At 100 microamperes

proton current, this is 700 per hour. It is obvious that background (such as positron annihilation radiation) in the X-ray measurements will be a problem. Hopefully, this can be reduced to a tolerable level: possibly the assumptions made are pessimistic ones. If not, the more complex, fast electron detection system will be required.

## 2. Diffusion studies

Another interesting, though very specific, utilization of the powder technique is in the investigation of the diffusion rate of atomic muonium in silica which in this instance may be considered as a light isotope of hydrogen. If a target of suitable particle size is used (that is, such that the average muonium diffusion time to the particle surface is about one microsecond), the time dependence of the asymmetry should have two components; one represents diffusion, the other the (fast) relaxation due to the low pressure oxygen environment. Such experiments will soon be undertaken at TRIUMF to elucidate the nature of the processes undergone by a muon in the powder target, and to investigate the effect of surface interactions on the muonium atom.

## 3. Chemistry of gases

One of the major efforts of the TRIUMF MSR group is the study of the chemical reactions of muonium atoms injected into a gas. The usual method is to stop the muons in an argon moderator, which supplies electrons necessary to muonium formation. Trace amounts of reactants are added to this moderator, and information on the reactions of muonium is drawn from the decay spectrum shape (relaxation, phase, etc.). However, since

the gas mixture of the target is at  $\sim 1$  atmosphere, the muons stop over a very large volume, hindering precise measurements. Moreover, the moderator itself may play some role in the reactions. Both of these problems might be largely alleviated with the use of a powdered moderator. This avenue is currently being explored at TRIUMF.

VI. Bibliography

Amato, J.J., P. Crane, V.W. Hughes, J.E. Rothberg, and P.A. Thompson, 1968, Phys. Rev. Lett. 21, 1709.

Bowen, T., K.R. Kendall, K.J. Nield, and A.E. Pifer, 1973, Lawrence Berkeley Laboratory Internal Report.

Brandt, W., and R. Paulin, 1968, Phys. Rev. Lett. 21, 193.

Brewer, J.H., D.G. Fleming, K.M. Crowe, R.F. Johnson, B.D. Patterson, A.M. Portis, F.N. Gygax, and A. Schenck, 1974, Physica Scripta 11, 144.

Cabot Corporation, Cab-O-Sil Properties and functions, 1976.

Danby, G., J-M. Gaillard, K. Goulianos, L.M. Lederman, N. Mistry, M. Schwartz, and J. Steinberger, 1962, Phys. Rev. Lett. 9, 36.

Eichten, T., H. Deden, F.J. Hasert, W. Krenz, J. Von Krogh, D. Lanske, J. Morfin, H. Weerts, G. Bertrand-Coremans, J. Sacton, W. Van Doninck, P. Vilain, D.C. Cundy, D. Haidt, M. Jaffre, G. Kalbfleisch, S. Natali, P. Musset, J.B.M. Pattison, D.H. Perkins, A. Pullia, A. Rousset, W. Venus, H. Wachsmuth, V. Brisson, B. Degrange, M. Haguenaer, L. Kluberg, U. Nguyen-Khac, P. Petiau, E. Bellotti, S. Bonetti, D. Cavalli, C. Conta, E. Fiorini, C. Franzinetti, M. Rollier, B. Aubert, L.M. Chounet, P. Heusse, A.M. Lutz, J.P. Vialle, F.W. Bullock, M.J. Esten, T.W. Jones, J. McKenzie, G. Myatt, and J.L. Pinfold, 1973, Physics Letters 46B, 281.

Feinberg, G., and S. Weinberg, 1961, Phys. Rev. 123, 1439.

Fleming, D.G., J.H. Brewer, D.M. Garner, A.E. Pifer, T. Bowen, D.A. Delise, and K.M. Crowe, 1976, J. Chem. Phys. 64, 1281.

Garner, D.M., J.H. Brewer, G. Clark, D.G. Fleming, G.M. Marshall, and J.B. Warren, to be published.

Gidley, D.W., P.W. Zitzewitz, K.A. Marko, and A. Rich, 1976, Phys. Rev. Lett. 37, 729.

Gurevich, I.I., I.G. Ivanter, E.A. Meleshko, B.A. Nikol'skii, V.S. Roganov, V.I. Selivanov, V.P. Smilga, B.V. Sokolov, and V.D. Shestakov, 1971, JETP 33, 253.

Hofer, H., K. Borer, P. Jenni, P. LeCoultre, P.G. Seiler, and P. Wolff, 1972, CERN research proposal.

Kendall, K.R., 1972, Ph.D. thesis, University of Arizona.

...cheva, G.G.,

Miyashcheva, G.G., Yu.V. Obukhov, V.S. Roganov, and V.G. Firsov, 1968, JETP, 26, 298.

Paulin, R., and G. Ambrosino, 1968, J. de Phys. 29, 263.

Pifer, A.E., T. Bowen, and K.R. Kendall, 1976, Nucl. Inst. and Meth. 135, 39.

Steltdt, F.R., and P.G. Varlashkin, 1972, Phys. Rev. B5, 4265.

West, R.N., 1973, Advances in Physics 22, 263.